

# An investigation of the reaction kinetics of luciferase and the effect of ionizing radiation on the reaction rate

Nikolas Berovic · David J. Parker · Michael D. Smith

Received: 4 August 2008 / Revised: 28 November 2008 / Accepted: 28 November 2008 / Published online: 18 December 2008  
© European Biophysical Societies' Association 2008

**Abstract** The bioluminescence produced by luciferase, a firefly enzyme, requires three substrates: luciferin, ATP and oxygen. We find that ionizing radiation, in the form of a proton beam from a cyclotron, will eliminate dissolved oxygen prior to any damage to other substrates or to the protein. The dose constant for removal of oxygen is  $70 \pm 20$  Gy, a much smaller dose than required to cause damage to protein. Removal of oxygen, which is initially in excess, leads to a sigmoidal response of bioluminescence to radiation dose, consistent with a Michaelis–Menten relationship to substrate concentration. When excess oxygen is exhausted, the response becomes exponential. Following the irradiation, bioluminescence recovers due to a slow leak of oxygen into the solution. This may also explain previous observations on the response of bioluminescent bacteria to radiation. We have studied the dependence of the reaction rate on enzyme and substrate concentration and propose a model for the reaction pathway consistent with this data. The light output from unirradiated samples decreases significantly with time due to product inhibition. We observe that this inhibition rate changes dramatically immediately after a sample is exposed to the beam. This sudden change of the inhibition rate is unexplained but shows that enzyme regulatory function responds to ionizing radiation at a dose level less than 0.6 Gy.

**Keywords** Protein · Ionizing radiation · Luciferase · Radiation damage · Oxygen depletion by radiation · Cooperativity

## Introduction

Luciferase is a firefly protein, responsible for the insect's ability to generate light. Since its discovery, it has been widely studied (Denburgh and McElroy 1970; McCapra and Beheshti 1985; Wood et al. 1989; Nakatsu et al. 2006; Vlasova and Ugarova 2007) and even more widely exploited (Henriquez et al. 2007; Xu et al. 2007; Harada et al. 2007). The catalytic activity of luciferase requires three substrates: luciferin, ATP and oxygen. The product of catalysis is an oxidised state of luciferin, a dioxetanone compound which is unstable. It emits a photon and decays into  $\text{CO}_2$  and oxyluciferin. Since the emitted light is a product that can easily be measured quantitatively, the luciferase reaction is particularly well suited for studies of enzyme catalytic mechanisms. Previously, we have investigated the effect of ionising radiation (Berovic et al. 2002) on the rate of luciferase bioluminescence. Our work raised several questions which could only be answered by a more detailed study of the mechanism of luciferase enzymatic activity. The present investigation therefore focuses both on the catalytic mechanism and the way that ionizing radiation affects various stages of the catalytic process.

In general, enzyme reaction rates can exhibit either sigmoidal or exponential forms of response to an increasing radiation dose. Human survival of whole body radiation doses is sigmoidal, a response which is also found in bioluminescent bacteria (Hug and Wolf 1956), but with the major difference that the sigmoid inflection for humans occurs at  $\sim 5$  Gy, while for bacteria it occurs at 150 Gy. The mechanism responsible for a sigmoidal response to radiation has been the subject of much speculation (Bacq and Alexander 1967). The sigmoidal response may suggest that low radiation doses have no effect and are therefore safe.

N. Berovic (✉) · D. J. Parker · M. D. Smith  
School of Physics and Astronomy,  
The University of Birmingham,  
Birmingham B15 2TT, UK  
e-mail: n.berovic@bham.ac.uk

On the other hand, enzyme damage is found to exhibit an exponential response to radiation when proteins are irradiated dry (Kepner and Macey 1968; Lidzey et al. 1995; Osborne et al. 2000). In this case, damage occurs due to direct collisions between protein molecules and the fluxes of primary particles and secondary electrons resulting from ionisation of the material in the target. If the total flux of all incident particles is  $\Phi$  and the cross-section of each molecule is  $\sigma$ , the number,  $N$ , of molecules that remain undamaged is given by:

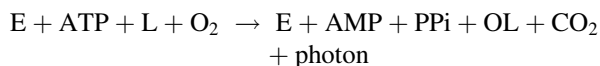
$$\frac{dN}{dt} = -\sigma \Phi N. \quad (1)$$

Since the radiation dose rate is linearly proportional to  $\Phi$ , Eq. 1 leads to an exponential dependence of survival on dose. This mechanism predicts that there is no safe dose, however small.

The issue was discussed by Lea (1962). The so-called Lea hypothesis suggests that in aqueous protein solutions, the response is sigmoidal due to an overwhelming primary interaction between radiation and water, leading to the formation of free radicals which subsequently react with protein. This cannot happen in dry samples, so that in this case damage to protein is a result of direct interactions between protein and incident particles.

We show below that aqueous solutions of protein can be made to exhibit both sigmoidal and exponential responses to radiation, therefore demonstrating that the Lea hypothesis is unsound. The issue can be understood only with reference to the details of the catalytic mechanism.

The essential facts about the luciferase bioluminescent reaction have been established for a long time (Wood et al. 1989). The protein luciferase (E) has molecular weight of 62 kD. Its structure has been determined (Conti et al. 1996; Nakatsu et al. 2006). The enzyme (E) binds adenosine-triphosphate (ATP) which is dephosphorylated to AMP. It also binds luciferin (L) and oxygen which ultimately leads to oxidation of luciferin into a dioxetanone compound (X) that is unstable (Kasney et al. 1983). This compound emits a photon and breaks up into carbon dioxide and oxyluciferin (OL).



Chemiluminescence from dioxetanones can be produced without catalysts, but in the case of luciferin, the presence of luciferase is necessary. The dependence of bioluminescence intensity on substrate concentrations obeys the usual Michaelis–Menten relation, as we confirm below. To explain the observation that the reaction rate depends quadratically on enzyme concentration, Ugarova et al. 1981, suggested that enzyme dimers are catalytically active rather than monomers. Our data lead us to suggest an alternative explanation.

A significant aspect of the reaction is that the rate of catalysis slows down with time after initial mixing. Since the initial concentrations of substrates are so high that they cannot be depleted rapidly, this slowing down must be due to “product inhibition” of the enzyme. Lemasters and Hackenbrock 1977, attributed the reduction in bioluminescence with time to the inhibitory effect of the product oxyluciferin on the enzyme activity. By investigating the change in light output when additional substrate was added to a mixture of enzyme and substrates which had been allowed to decay, they showed that the product inhibition is noncompetitive with respect to both luciferin and ATP substrates. Our data confirm the importance of this product inhibition, but also reveal unexpected features. In particular, sudden changes of inhibition rate at the start of irradiation remain unexplained.

## Materials and methods

The luciferase used was from *Luciola mingrelica* (SIGMA L 4899) and shows identical response to radiation as the luciferase from *Photinus Pyralis* which we used previously (Berovic et al. 2002). It was diluted in a buffered solution: HEPES (SIGMA H 7523) 25 mM at pH 7.8, containing 5 mM DTT (SIGMA D5545). The protein concentration was normally 6  $\mu\text{g/ml}$  (0.1  $\mu\text{M}$ ) except when the dependence on enzyme concentration was investigated. All concentrations are based on the manufacturer’s specifications.

Substrates were made in the same buffer with 2 mM luciferin (SIGMA L6882), 5 mM ATP (SIGMA A7699) and 15 mM  $\text{MgCl}_2$ . Oxygen from air is normally dissolved in water at a concentration of about 5 ppm (0.3 mM).

Dilution experiments were performed keeping the concentration of all other reactants strictly constant.

Irradiation was performed on the University of Birmingham MC40 cyclotron, using proton beams of energy 15 and 30 MeV. The lower energy was used with a 0.3 mm thick target, while the 30 MeV beam was used with a 3 mm thick target. The specific energy losses of the two beams were 3 and 2 keV/micron, respectively. Beam currents ranged from 20 to 150 pA. Low currents were employed in order to obtain clear evidence of the low dose, flat part of the sigmoid response of bioluminescence to radiation. The beam was brought from an evacuated beam line into air through a 0.03 mm *havar* window. Currents were monitored on collimators and measured by a magnetically suppressed Faraday cup mounted in air at the position subsequently occupied by the target, adjacent to the exit window. For the 3 mm target, solutions were contained in a *perspex* ring which enclosed a circle 10 mm diameter which formed the target volume. This ring was accurately positioned after the exit window aligned to the

proton beam which was defined by collimators and had a diameter of 10 mm. The uniformity of the beam over the area of the target was checked using *radiochromic* films. The front and back faces of the *perspex* ring were enclosed with foils of *mylar* 0.01 mm thick, aluminized on the outer face. Clamps and silicone grease ensured that the sample volume was water tight. The aluminium coating acted as a reflector of light emitted by the solution within the target volume. Most of the light emerged through the sides of the ring. An optical fibre coupled to the *perspex* ring transmitted some of the light to the photo-cathode of a photomultiplier (EMI 9893/100). This enabled simultaneous monitoring of enzymatic activity during irradiation. The photomultiplier was operated in photon counting mode, and the numbers of counts in 0.5 or 1 s intervals were recorded to provide a record of light intensity as function of time, prior, during and after irradiation.

The 0.3 mm thick target was previously described (Berovic et al. 2002) when agarose was used to provide a solid matrix that contained the solution of reactants. In the present experiment the solution was pure liquid without agarose.

An incident proton beam of 20 pA or more caused the solution to scintillate due to ionization of molecules in the solution, in addition to the emission of bioluminescence. The beam-induced scintillation corresponded to around 5,000 cps compared to up to 500,000 cps due to bioluminescence, and contributed a constant pedestal in count rate during beam-on time, which could subsequently be easily subtracted.

To measure the effect of radiation on the concentration of oxygen dissolved in water, a rectangular (4 × 4 mm, 3 mm thick) target chamber was made in *perspex* with *mylar* faces front and back. A platinum electrode was introduced into one side of the chamber and sealed with varnish. The other side was in contact with a compartment which contained 3 M KCl solution and a silver electrode. This chamber and target were separated by a plain *mylar* foil 0.01 mm thick which was permeable to the current making a Pt–Ag/AgCl electrolytic cell. A negative bias of –1 V applied to the Pt electrode produced a current of a few microamperes which declined to 1 μA as the Pt electrode became polarised. The stationary current is due to creation of O<sup>•–</sup> ions at the Pt electrode; hence it depends on diffusion of oxygen towards the Pt electrode. This process is sensitive to the oxygen concentration in the target volume. Bubbling nitrogen or oxygen gases through the water was found to alter the current in proportion to the change of concentration of dissolved oxygen (data not shown).

## Experimental data

In the first instance, we have studied the luciferase reaction kinetics without the intervention of ionizing radiation. The

response to variation of the concentration [L] of the substrate luciferin is shown in Fig. 1.

The data in Fig. 1 include a background of 100 cps due to contamination. After normalizing to unity at maximum count rate, they are fitted by the expression:

$$I_L = \frac{1}{1 + \exp[-(g + \ln[L])]}; \quad g = 7.5. \quad (2)$$

Dependence on the enzyme concentration was investigated under two different protocols, both of which produced a sequence of enzyme dilutions while keeping the substrate concentration constant: (I) Enzyme pre-reaction dilution, where the enzyme was first diluted with buffer to form a sequence of concentrations. Each diluted enzyme solution was then separately combined with substrates that were at fixed concentration. (II) For mid-reaction dilution, the enzyme was combined with substrates and while the reaction proceeded, aliquots of this solution were taken at 10 min intervals and diluted further with substrate solution, and the resulting bioluminescence count obtained. This protocol examined whether the role of enzyme differs in the later stages of the reaction.

Data for the two protocols are shown in Figs. 2 and 3.

In both cases, the mathematical expression that represents data for the reaction rate in terms of enzyme concentration [E] is:

$$Y = \frac{([E]/C)^n}{1 + ([E]/C)^n}, \quad C \approx 10^{-7}. \quad (3)$$

In the limit [E] < C (when saturation is unimportant), the reaction rate  $Y \sim [E]^n$ . The exponent,  $n$ , differs

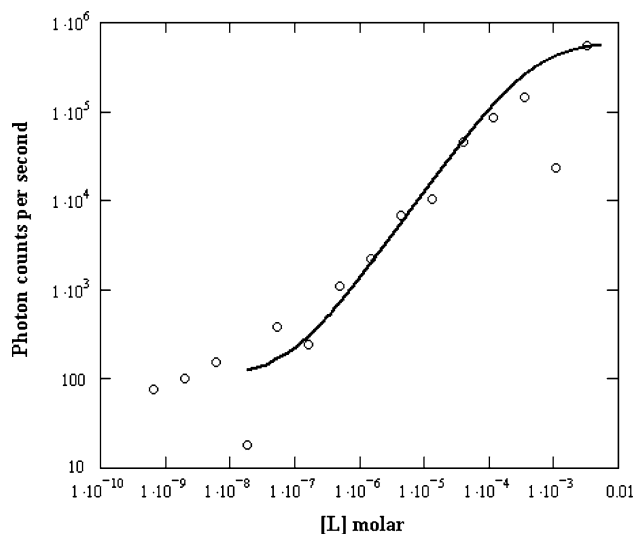


**Fig. 1** Light intensity of the initial bioluminescence measured for different concentrations [L] of luciferin (*open circle*). The solid line shows the Michaelis–Menten fit (Eq. 2)

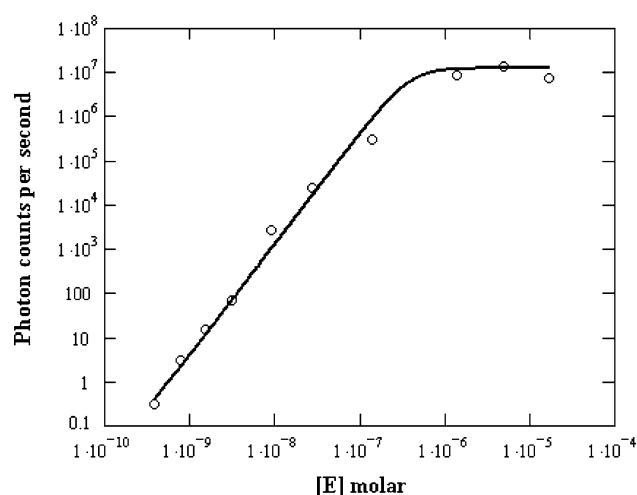


**Fig. 2** Light intensity of the initial bioluminescence for different initial concentrations  $[E]$  of the enzyme (*open circle*). Enzyme dilution was performed according to protocol I. The *solid curve* shows the fit obtained with Eq. 3 using the parameters given in the text

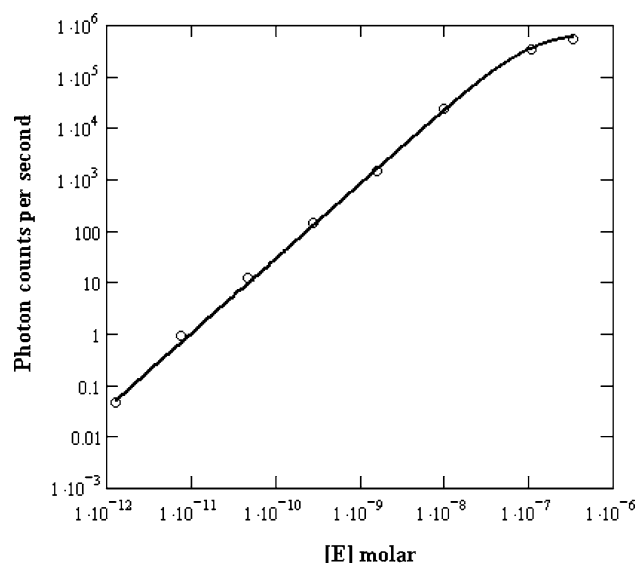


**Fig. 3** Light intensity of the initial bioluminescence for different concentrations  $[E]$  of the enzyme obtained by subsequent dilution of the reaction mixture using protocol II. The *solid curve* shows the fit obtained with Eq. 3 using the parameters given in the text

between the two dilution protocols. For pre-reaction dilution,  $n = 2.5$ . For mid-reaction dilution,  $n = 1.5$ – $1.7$ .

We note that  $n$  is never unity; enzyme–enzyme collisions always play a part even when the reaction has been going for a long time. The value  $n = 2.5$  shows that a significant pathway involves three enzyme collisions. The fact that the exponent changes by one unit, from  $n = 2.5$  to  $n = 1.5$ , upon mixing enzyme with substrates, suggests that one enzyme collision takes place rapidly, followed by much slower steps along the pathway, where enzyme–enzyme collisions still take place an hour after the reaction

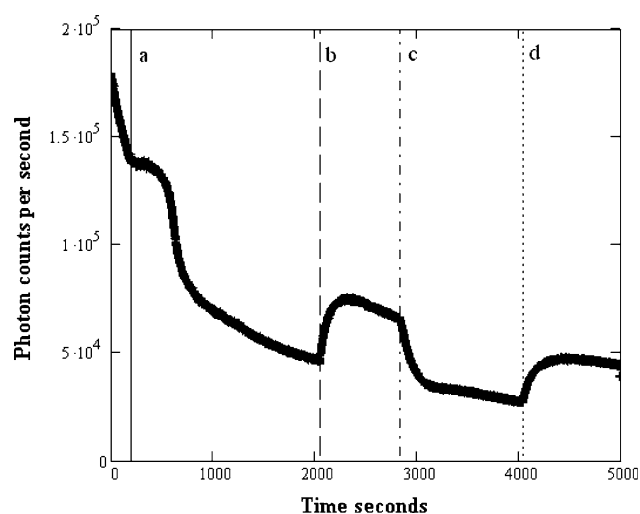


**Fig. 4** Light intensity of the bioluminescence prior to, during and after irradiation by the proton beam. The beam was applied in two dose fractions, between points *a* and *b*, and between points *c* and *d*. During the periods when the beam was on, scintillation due to ionization contributed a constant 5,000 cps background which has been subtracted from the data. The data show both sigmoidal and exponential responses to radiation, and exponential recovery when the beam was switched off

started. It is natural to assume that the first rapid step involves binding of an enzyme molecule to any one of the three substrates.

Irradiation of actively bioluminescing solutions using the proton beam from the cyclotron was performed as described in the experimental methods. An example of the effect of ionizing radiation on the catalytic rate is shown in Fig. 4. From the start, the light output from the unirradiated sample decreases exponentially with time as  $\exp(-t/t_1)$ , due to the product inhibition (Lemasters and Hackenbrock 1977). For all unirradiated samples, the inhibition time constant,  $t_1$ , was found to have a value of 500–750 s, approximately independent of enzyme concentration.

Two fractions of radiation dose were delivered to the sample in Fig. 4, separated by a period when the beam was off, during which bioluminescence showed recovery. The timing of the two dose fractions is shown in Fig. 4 by vertical lines. A constant background of 5,000 cps due to scintillation of the solution has been subtracted from the data during beam-on times.

The most obvious feature of the data is that during the first fraction of radiation dose, the response is sigmoidal, while during the second fraction it is exponential. In both cases, the overall effect is to reduce the bioluminescence by a factor of approximately 50%. An exponential recovery occurs when the beam is switched off, with a time constant  $T \sim 100$  s.

The next point to note is the immediate change of the inhibition rate when the beam strikes the sample. From the

value of  $t_i = 750$  s, the inhibition slows down to  $t_i = 15,000$  s.

The effect of irradiation is superimposed on the reduction in activity due to product inhibition. It is difficult to tell whether the radiation causes any permanent damage to the enzyme. The overall impression is that the recovery after irradiation approximately restores the bioluminescence to the level which would have been found if no irradiation had occurred.

Fitting a sigmoidal function to the data from the first dose fraction reveals that the sigmoid inflection point occurred after a time,  $T_i = 435 \pm 20$  s. The uncertainty is primarily due to ambiguities in the fitting procedure in the presence of inhibition. Assuming a dose rate of 0.6 Gy/s, which corresponds to the 15 MeV proton beam, current of 20 pA and target 0.3 mm thickness, the dose received up to the inflection point was  $260 \pm 15$  Gy. The data shown in Fig. 4 correspond to an enzyme concentration of 6  $\mu\text{g/ml}$ . The experiment was repeated using a range of enzyme concentrations, and very similar results were observed, except that the irradiation time necessary to reach the sigmoid inflection point reduced slightly with increasing enzyme concentration, as shown in Fig. 5. The full line in Fig. 5 is  $T_i = 450 - 18 \ln[E]$ .

Further tests were conducted to identify the origin of these effects:

- Pure enzyme was irradiated alone to 300 Gy. This enzyme showed no decrease of catalytic activity when subsequently combined with unirradiated substrates, relative to the activity of fresh enzyme.
- A solution of luciferin and ATP was irradiated on its own to 300 Gy and showed no decrease in activity when combined with unirradiated enzyme.

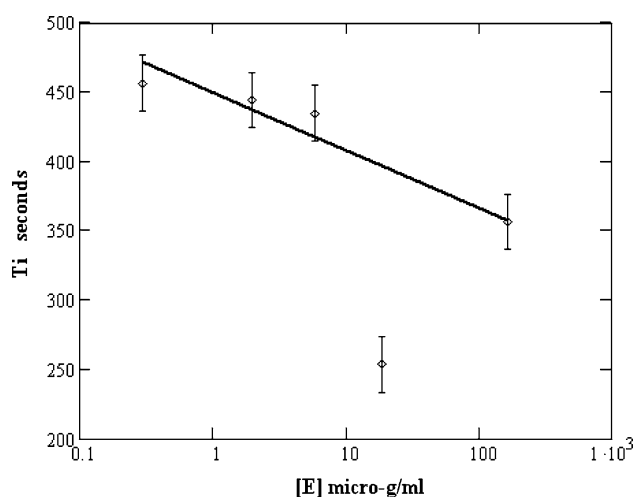


**Fig. 5** Variation of  $T_i$  (the time of irradiation by the proton beam necessary to reach the inflection point of the sigmoid response) with enzyme concentration. The solid line shows the relationship  $T_i = 450 - 18 \ln[E]$

We conclude that damage to protein, ATP and luciferin are not of primary importance.

- Since the solution within the target volume is isolated from the air, any removal of oxygen would not be quickly replenished. To find if oxygen was depleted by radiation following the first fraction of radiation, the target volume was opened to air allowing oxygen to dissolve in the solution for 5 min, before re-sealing the target and delivering the second dose fraction. The results in Fig. 6 show that a sigmoidal dose-response was restored by exposing the previously irradiated target to unrestricted ingress of oxygen. A third dose fraction was then delivered, where the target remained sealed between the second and third dose fractions, and showed an exponential response. These results suggest that the difference between the sigmoidal and exponential responses can be entirely attributed to the concentration of dissolved oxygen. The applied dose during the first fraction significantly reduces the oxygen concentration within the target volume. While it remains low, subsequent dose fractions show an exponential dose dependence.

We show later that the recovery of bioluminescence after irradiation can also be attributed to the recovery of oxygen concentration. This happens due to leaking of oxygen gas into the target due to an imperfect seal.

Not shown in this figure is a fourth exposure to radiation which took place at 3,500 s. The target was not interfered

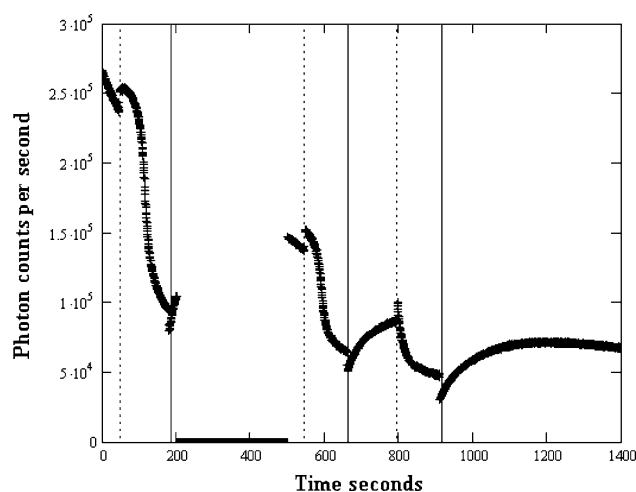


**Fig. 6** Intensity of the bioluminescence prior to, during and after three fractions of radiation dose separated by periods of recovery. The start of each fraction is denoted by a dotted marker and the end by a solid marker. For the purpose of illustration, the background of scintillation photons has not been subtracted from these data. Between fractions 1 and 2, the solution was exposed to air during the period shown by zero counts. The ingress of oxygen restored the sigmoidal response during the second fraction of dose. The third fraction shows exponential response as expected when oxygen has been depleted by the preceding radiation dose



between the third and fourth fractions of radiation dose, but a long time ( $\sim 1,500$  s) was allowed for oxygen recovery between dose deliveries. Prolonged recovery of oxygen concentration was sufficient to restore a sigmoid response in the fourth fraction of dose.

To verify these conclusions, two further tests were conducted:

- (d) A combined solution of enzyme and substrates, before being placed in the target was placed in a nitrogen filled glove-box. A stream of nitrogen gas was bubbled for 2 min through the solution, depleting the oxygen concentration in the solution. In the glove-box, the solution was transferred into the target volume, sealed and subsequently placed in the beam. The results for this hypo-oxygenated target are shown in Fig. 7.

During the first fraction of radiation and for subsequent fractions, this hypo-oxygenated solution gives an exponential dose-response. Following irradiation, in Fig. 7, can be observed an increase of bioluminescence due to the leak of air into the target. At the point 1,200 s after the start, the mylar faces of the target were punctured allowing easy access of air to the target solution. This clearly resulted in a rapid recovery of bioluminescence, as the oxygen level in the solution reached the normal level of 5 ppm in equilibrium with the atmosphere. The bioluminescence intensity rose to exceed the intensity at the start when the solution was hypo-oxygenated. The reaction mechanism then comes into play to limit further increase of the reaction rate.

- (e) These results strongly suggest that the concentration of dissolved oxygen is significantly reduced due to the irradiation by the beam. This conclusion was verified

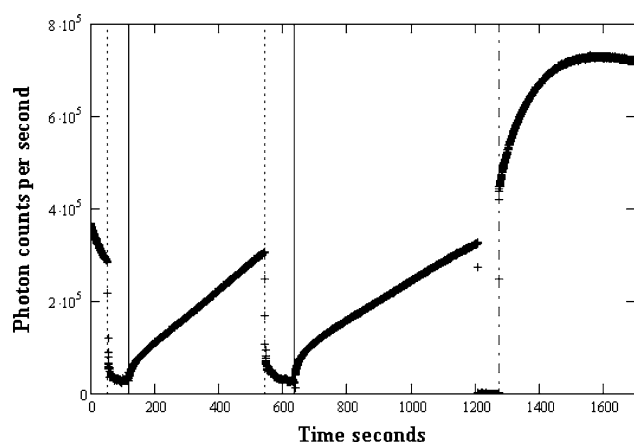


**Fig. 7** Light intensity of the bioluminescence when two fractions of radiation dose were delivered to a hypo-oxygenated target. The start of each fraction is denoted by a dotted marker and the end by a solid marker. Both fractions elicit exponential response. After 1,200 s, the target seal was punctured to allow access of oxygen to the solution: the data following the dot-dash marker show the corresponding recovery in bioluminescence due to reoxygenation

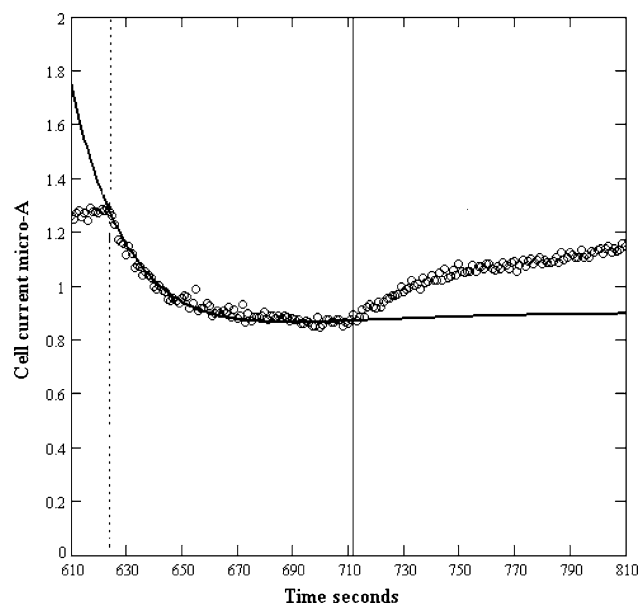


**Fig. 8** Electrolytic current from the Pt–Ag/KCl cell which contained pure water (open circles). A single fraction of radiation by the proton beam, delivered between the points shown by the dotted and solid markers, elicited exponential response. The solid curve shows an exponential fit with time constant  $1/35 \text{ s}^{-1}$

directly by an independent measurement of the oxygen concentration during irradiation. A target which contained pure water was irradiated while monitoring the concentration of dissolved oxygen by oxygen-sensitive polarography as described in the section “Methods”. The current between the Pt and Ag/KCl electrodes is proportional to the concentration of oxygen in the target. A 30 MeV proton beam of 20 pA produced the exponential decay of electrolytic current shown in Fig. 8 followed by recovery when the beam was switched off. The dose rate for this irradiation was 2 Gy/s.

The data can be fitted using a rate constant for oxygen removal  $w = 1/35 \text{ s}^{-1}$  which amounts to a dose constant  $D_0 = 70 \pm 20 \text{ Gy}$ . The uncertainty arises from ambiguities in parameter fitting.

## Discussion

The data for dependence of bioluminescence intensity,  $I$ , on initial enzyme concentration  $E_0$ , under two protocols, show that the first encounter between enzyme and one substrate occurs rapidly, but that subsequent steps along the reaction pathway require one to two more enzyme–enzyme encounters. Since these steps are slow, the first step will reach a quasi-equilibrium. Hence, it is reasonable to expect that the reaction rate,  $V$  can be described in terms of any

substrate concentration  $[S]$  by the standard Michaelis–Menten form:

$$V = \frac{V_{\max}[S]}{K_m + [S]}. \quad (4)$$

This expression is indeed identical to Eq. 2 which was used to fit the dependence on luciferin concentration, if the following substitutions are made.  $V_{\max} = 1$ ,  $K_m = \exp(-g)$ . The value,  $g = 7.5$  from this fit implies a value  $K_m = 4 \times 10^{-5}$  M for the reaction of enzyme with luciferin.

We have already demonstrated that the primary effect of irradiation is to reduce the concentration of dissolved oxygen. The direct measurement of oxygen concentration as a function of radiation dose,  $D$  (Fig. 7) shows concentration falling exponentially with radiation dose,  $D$  (or irradiation time,  $t$ ). Neglecting any replenishment due to leakage of oxygen into the target and substituting  $[O_2] = O_0 \exp(-wt)$  into the Michaelis–Menten equation would give the expression.

$$V = \frac{V_{\max}}{1 + \frac{K_m}{O_0} \exp(wt)} \quad (5)$$

Provided the initial oxygen concentration  $O_0 \gg K_m$ , this expression is sigmoidal. Initially  $V \approx V_{\max}$  (constant). As the oxygen concentration reduces, an inflection occurs when  $[O_2] = K_m$ . Subsequently, when  $[O_2] \ll K_m$ ,  $V \approx \frac{V_{\max}O_0}{K_m} \exp(-wt)$ .

Hence, substituting an exponentially decreasing oxygen concentration into the Michaelis–Menten equation can predict either sigmoidal or exponential variation in enzyme activity, depending on the initial concentration of oxygen.

The expressions above predict activity reducing to zero at large time. In contrast, our data show that the effect of irradiation is to reduce the enzyme activity only by around 50%. This phenomenon can also be explained by allowing for the simultaneous leakage of oxygen into the target. Then the rate of change of oxygen concentration can be described in terms of the radiation damage rate,  $w$ , and the leak rate,  $l$ , by:

$$\frac{d}{dt}[O_2] = -w[O_2] + l(O_0 - [O_2]) \quad (6)$$

where  $O_0 = 3 \times 10^{-4}$  M, is the initial oxygen concentration when the solution is in equilibrium with air. The analytical solution of this equation is  $\frac{O_0}{w+l} [w \exp(-(w+l)t) + l]$ , which shows  $[O_2]$  falling exponentially with rate constant  $(w+l)$  towards a limiting concentration  $O_\infty = \frac{l}{w+l} O_0$ , at which the leakage and damage rates balance. Substituting the analytical solution into the Michaelis–Menten equation leads to an expression for the enzyme reaction rate which tends to  $\frac{V_{\max}}{1 + K_m/O_\infty}$  at large dose. This

limit can be approached either sigmoidally or exponentially, depending on the initial oxygen concentration. After

irradiation, this model predicts exponential recovery of activity due to the leakage rate,  $l$ .

When the sample is in equilibrium with the air, the oxygen concentration greatly exceeds  $K_m$ , providing a buffer for the intermediate  $EO_2$ , and so initial depletion of oxygen by irradiation has no effect on the reaction rate. Only when the concentration is reduced to a value close to  $K_m$ , does the reaction rate fall. Thereafter the enzymatic activity closely follows the oxygen concentration, showing exponential recovery following irradiation and exponential decay, if a second irradiation is applied to the hypoxic solution. Only after about 25 min does the oxygen concentration recover to a level where a sigmoidal response is again seen.

It appears therefore that this model could provide a complete description of the results for bioluminescence versus dose, using appropriate values for the parameters  $w$ ,  $l$  and  $K_m$ . A typical fit to the first radiation dose is shown in Fig. 9.

However, attempts to fit a complete sequence of irradiations and recovery such as those in Fig. 4 are complicated by the simultaneous presence of the non-competitive product inhibition process. The Michaelis–Menten form of reaction rate generates buffering due to the excess of substrate with respect to free enzyme, but remains sensitive to the enzyme concentration: if the final reaction products remain bound to the enzyme, they decrease the available enzyme concentration and the

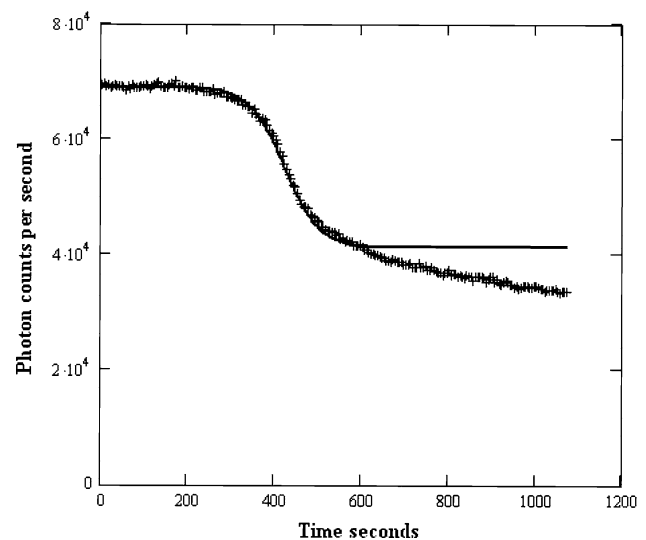


**Fig. 9** Intensity of the bioluminescence during the first fraction of radiation dose (*plus*). For clarity only every tenth data point is plotted. The *solid curve* shows the fit obtained using the Michaelis–Menten form for reaction rate (Eq. 5), where the dependence of oxygen concentration on dose is obtained from Eq. 6. This theory does not take account of the product inhibition. Apparently the time constant for product inhibition has changed from 15,000 s at the start of irradiation to 1,700 s after the sigmoid transition

reaction slows down. This process could be included in the above equations, but not in a way that accounts for the variations in inhibition rate discussed below.

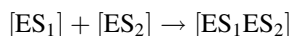
A further problem is that to achieve quantitative fits to both radiation doses and recovery of the bioluminescence response, it is necessary to make unphysical changes to the parameters  $w$ ,  $l$  and  $K_m$ .

These limitations are unsurprising, since the model provides an incomplete description of the entire catalytic process. It fails in three aspects: (1) the dependence of reaction rate on  $E_0^{2.5}$  (Fig. 2), (2) the data which show decrease of buffering capacity with  $E_0$  (Fig. 5), and (3) the sudden change of the inhibition rate constant, when the beam strikes the target.

The simple assumption that the reaction proceeds via a linear process  $E + S_1 + S_2 + S_3 \rightarrow ES_1S_2S_3$  is excluded by the  $n = 2.5$  dependence of Fig. 2. The power dependence on  $E_0$  could be obtained if one assumed that the monomer  $ES_1S_2S_3$  is completely inactive and dimers are the active oligomers, as already suggested by Ugarova et al. (1981) who obtained data with  $n = 2$ .

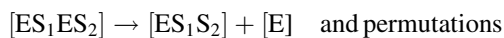
However, any scheme that involves dimers and trimers also needs to explain the data in Fig. 5. These show that the dose required to exhaust the buffering capacity of  $[EO_2]$  decreases with increasing enzyme concentration  $E_0$ , in a logarithmic fashion. To achieve that, the slow step which creates  $[EO_2]$  must be followed by reactions in which enzyme again participates, so that outflow from the buffering reservoir is greater when there is more enzyme present.

A reaction pathway which gives the correct buffering and power law could be:

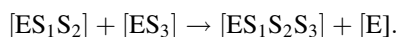


and permutations with  $S_1, S_3$  and  $S_2, S_3$

...



...



In this proposal the monomer,  $ES_1S_2S_3$ , is active and proceeds to catalyze luciferaladenylate into dioxetanone.

We have confirmed that numerical solution of the entire system of differential rate equations given by this reaction scheme behaves as required. This scheme avoids the awkward requirement that monomers are totally inactive. It is consistent with our data for dilution of enzyme using protocol II, which showed an exponent  $n = 1.5$  for the dependence on enzyme concentration after the reaction had been going for some time. The scheme is also consistent

with the X-ray data of Nakatsu et al. (2006) who grew crystals of luciferase, identifying all three substrates bound to monomers.

For an enzyme tightly packed within “oocytes” as luciferase in fireflies, there is some sense in the facility to pass on substrates from one to the other monomer which amounts to a form of cooperativity.

The model should also incorporate product inhibition of enzyme activity. Lemasters and Hackenbrock (1977), found that this inhibition is noncompetitive with respect to the substrates luciferin and ATP. It is instructive to compare quantitatively the rate of product formation with the number of molecules of enzyme present in order to ascertain whether these numbers can account for the observed inhibition. Because of uncertainty in the light collection efficiency, this can only be done approximately in the present study. We estimate that the number of product molecules generated during the initial 200 s prior to irradiation will produce an inhibition rate which is  $10\times$  lower than actually observed, even if we assume that every product remains bound to an enzyme molecule leaving it inactive for a long time.

This unsatisfactory aspect is further aggravated by the failure of the model to give even a qualitative explanation for the sudden changes of inhibition observed when the proton beam strikes the sample. The data show that the light intensity does not change, but the rate of inhibition reduces dramatically. In Fig. 4, one can see that during the first dose, the inhibition time constant (previously 750 s) changes almost instantly (within 1 s) to approximately 15,000 s. After the sigmoid transition, it returns to approximately 1,700 s, and remains similar during the second dose (2,200 s.) It appears that, when the beam starts, the proportion of enzyme which is already inhibited remains unchanged but for some unexplained reason, products from subsequent reactions have a greatly reduced inhibitory effect, a change which affects the entire population of enzyme molecules in the target. This change is produced by a dose  $<0.5$  Gy. This is surprising when compared to the dose necessary to impair the enzyme catalytic function ( $>1,000$  Gy). The regulatory function of product inhibition in controlling the operation of the enzyme appears to be very sensitive to radiation. Attempts to determine the cross-section are subject to a large uncertainty due to sensitivity to the range-energy spectrum of secondary electrons, but estimates suggest that the regulatory function may have a cross-section for interaction with the total flux of protons and secondary electrons which is bigger than the size of a single protein molecule.

The above model also fails to account for the saturation at high enzyme concentrations and the dependence of quantum efficiency on enzyme concentration,  $E_0$ , which



declines from 90% at high concentration to lower values at low concentration (Chittock et al. 1993).

## Conclusions

Our data provide an explanation for the observed sigmoid and exponential responses of enzyme catalytic rate to ionizing radiation. The rate of depletion of oxygen by radiation is far greater than either that of the protein or the other substrate molecules. The ionizing radiation removes dissolved oxygen and this governs the entire cycle of bioluminescence responses observed in Fig. 4.

This evidence is sufficient to account for the results on the response of bioluminescent bacteria to radiation (Hug and Wolf 1956). At similar dose levels to those we used for luciferase reaction in vitro, bacteria showed a sigmoidal fall of bioluminescence which corresponds to oxygen removal by radiation. The recovery of bacterial bioluminescence after irradiation was observed, similar to that shown by our samples. Evidently the protein function remained undamaged while the oxygen concentration recovered. Thus there is a quantitative correspondence between the way protozoa respond to radiation and protein responds in vitro. The case of mammalian response is an entirely different matter, where the sigmoid inflection occurs at 4–5 Gy.

We have only been able to give a partial account of the data relating to the luciferase reaction mechanism. In particular the changes in the time constant for product inhibition are unexpected and show that the regulatory side of protein function is very sensitive to ionizing radiation.

**Acknowledgments** We wish to acknowledge the support of EPSRC.

## References

- Bacq ZM, Alexander P (1967) Fundamentals of radiobiology, 2nd edn. Pergamon Press, Oxford
- Berovic N, Pratontep S, Bryant A, Montouris A, Green RG (2002) The kinetics of radiation damage to the protein luciferase and recovery of the enzyme activity after irradiation. *Radiat Res* 157:122–127. doi:10.1667/0033-7587(2002)157[0122:TKORDT]2.0.CO;2
- Chittock RS, Lidzey DG, Berovic N, Wharton CW, Jackson JB, Beynon TD (1993) The quantum yield of luciferase is dependent on ATP and enzyme concentrations. *Mol Cryst Liq Cryst (Phila Pa)* 236:599–604. doi:10.1080/10587259308055210
- Conti E, Franks NP, Brick P (1996) Crystal structure of firefly luciferase throws light on a superfamily of adenylate-forming enzymes. *Structure* 4:287–298. doi:10.1016/S0969-2126(96)00033-0
- Denburgh JL, McElroy WD (1970) Catalytic subunit of firefly luciferase. *Biochemistry* 9:4619–4624
- Harada H, Kizaka-Kondoh S, Li G, Itasaka S, Shibuya K, Inoue M, Hiraoka M (2007) Significance of HIF-1<sub>α</sub> active cells in angiogenesis and radioresistance. *Oncogene* 26:7508–7516. doi:10.1038/sj.onc.1210556
- Henriquez NV et al (2007) Advances in optical imaging and novel model systems for cancer metastasis imaging. *Clin Exp Metastasis* 24(8):699–705. doi:10.1007/s10585-007-9115-5
- Hug O, Wolf I (1956) Progress in radiobiology. Oliver and Boyd, Edinburgh, p 23 (see also Bacq and Alexander 1967, chapter 14, p 375)
- Kasney M, Pamuk HO, Trindle C (1983) A MINDO/3 study of the properties of the ground state dioxetanone molecule and its dissociation potential energy surface into CH<sub>2</sub>O + CO<sub>2</sub> Theorchem-. *J Mol Struct* 13:459–470
- Kepner GR, Macey RI (1968) Membrane enzyme systems—molecular size determinations by radiation inactivation. *Biochim Biophys Acta* 163:188–203. doi:10.1016/0005-2736(68)90097-7
- Lea DE (1962) Actions of radiations on living cells. Cambridge University Press, London
- Lemasters JJ, Hackenbrock CR (1977) Kinetics of product inhibition during firefly luciferase luminescence. *Biochemistry* 16:445–447. doi:10.1021/bi00622a016
- Lidzey DG, Berovic N, Chittock RS, Beynon TD, Wharton CW, Jackson JB, Parkinson N (1995) A critical analysis of the use of radiation inactivation to measure the mass of protein. *Radiat Res* 143:181–186. doi:10.2307/3579155
- McCapra F, Beheshti I (1985) Selected chemical reactions that produce light in bioluminescence and chemiluminescence, vol 1. CRC Press, Boca Raton
- Nakatsu T, Ichiyama S, Hiratake J, Saldanha A, Kobashi N, Sakata K, Kato H (2006) Structural basis for the spectral difference in luciferase bioluminescence. *Nature* 440:372–376. doi:10.1038/nature04542
- Osborne JC, Miller JH, Kempner ES (2000) Molecular mass and volume in radiation target theory. *Biophys J* 78:1698–1702
- Ugarova NN, Brovko LI, Beliaeva EI et al (1981) Dimers are catalytically active particles of glowworm luciferase. *Dokl Akad Nauk SSSR* 260(2):358–360
- Vlasova TN, Ugarova NN (2007) Quenching of the fluorescence of Tyr and Trp residues of firefly luciferase from *Luciola mingrelica* by the substrates. *Biochemistry (Mosc)* 72:962–967
- Wood KV, Lam YA, McElroy WD (1989) Introduction to beetle luciferases and their applications. *J Biolumin Chemilumin* 4:289–301
- Xu XD et al (2007) Imaging protein interactions with bioluminescence resonance energy transfer (BRET) in plant and mammalian cells and tissues. *Proc Natl Acad Sci USA* 104(24):10264–10269. doi:10.1073/pnas.0701987104